



Title:

**Stress Constrained Topology Optimization for Lattice Structures**

Authors:

Yiding Sun, yiding1@ualberta.ca, University of Alberta

Xinming Li, xinming1@ualberta.ca, University of Alberta

Yongsheng Ma, mays@sustech.edu.cn, Southern University of Science and Technology

Keywords:

Topology Optimization, Stress Constraint, Lattice Structure, Medical Engineering

DOI: 10.14733/cadconfP.2024.57-62

Introduction:

Significant strides in additive manufacturing have enabled the production of cellular structures with intricate geometries [1]. Topology Optimization (TO), a practical design tool, has been extensively associated with additive manufacturing due to its ability to generate novel and unforeseen designs [2,3]. These designs find utility across diverse applications, including medical engineering [4], automotive [5], aerospace [6], biomechanics [7], and energy industry [8]. Reducing the weight of a component under stress constraints could maximize the strength-to-weight ratio of the component, which has been a pivotal objective in practical industries. The study investigates the stress constraints within TO, a field where numerous classical approaches have been proposed to tackle challenges in stress-based TO [9,10]. Moreover, the stress-based TO methodology is extended to other material fields like multiple isotropic materials, anisotropic materials, and hyperelastic materials [11,12]. By combining the TO method with the homogenization approach, the material distribution in multiscale is properly tailored, and the structures with enhanced mechanical performance are achieved. In light of its significance, stress constraints have been investigated within the multiscale TO frameworks [13].

The emulation of bone-like structures in the architectural design of medical engineering presents a compelling avenue for innovation and efficiency. Bone is composed of compact cortical bone and spongy cancellous bone, which form its outer shell and interior. This composite structure arises from a natural optimization process aligning with Wolff's law [14]. Several methodologies have been proposed to emulate and optimize bone-like structures. Liu and Shapiro [15] introduced a technique for reconstructing 3D microstructures from 2D samples based on example-based texture synthesis, which could preserve given statistical features. Another study emphasized anisotropic filtering that directs material accumulation in preferred orientations, resembling bone-inspired infills, resulting in enhanced stiffness and robustness [14,16]. Additionally, Daynes et al. [17] aligned lattice trusses with principal strain directions to increase the stiffness and intensity of structures. Whereafter they proposed a bio-inspired approach that integrates topology and size optimization, resulting in promising applications across multiple loading case scenarios [18]. However, other than the mechanical performance challenges faced in the design for additive manufacturing, computationally economical solutions for mass-customized medical engineering problems are still scarce. This work aims to propose the stress-constrained TO method for lattice structures. By extending the ordered Solid Isotropic Material with Penalization (SIMP) like stress interpolation to the composite material criterion, multiple microstructure distributions can be determined on the macroscale. In particular, the Tsai-Hill yield criterion-based constraint expression is established in this work. This attribute presents considerable potential in

enhancing mechanical performance, alleviating the structural design complexity, and concomitantly augmenting safety protocols.

### Algorithm Framework

A model is established to ensure the consistency of the yield strength on the microscale, and the stresses calculated by the homogenized model on the macroscale. Therefore, the multiscale failure model is employed to qualify the yield strength of lattice structure with a predefined density ratio. Based on this model, an ordered SIMP stress interpolation is constructed, and a so-called scaling method is adopted to realize the stress constraints for different microstructures through a global constraint. For simplicity, in the remaining content of this subsection, the problem is addressed under 2 D orthogonal-isotropic microstructures.

### Ordered SIMP Stress Interpolation

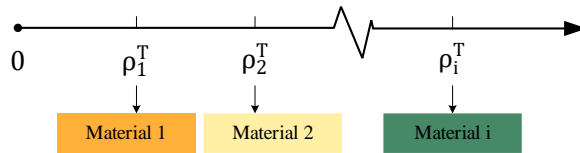


Fig. 1: Illustration of density-based material sorting.

The ordered SIMP method is employed to evaluate the properties of composite materials. As depicted in 0, the pseudo isotropic materials are sorted in the ascending order of the material density  $\rho_i^T$ . Considering the anisotropic properties of the lattice structures, the homogenization elastic tensor for the element  $e$  ( $\mathbf{D}_e$ ) could be expressed as:

$$\mathbf{D}_e = \boldsymbol{\eta}^E \cdot \mathbf{D}_{\max}^H, \quad (2.1)$$

$$\boldsymbol{\eta}^E = \left( \frac{\rho_e - \rho_i^T}{\rho_{i+1}^T - \rho_i^T} \right)^p \cdot \left( \frac{\mathbf{D}_{i+1}^H - \mathbf{D}_i^H}{\mathbf{D}_{\max}^H} \right) + \frac{\mathbf{D}_i^H}{\mathbf{D}_{\max}^H}, \quad (2.2)$$

where  $\mathbf{D}_i^H$  is the effective elastic tensor which can be calculated by the homogenization method,  $\mathbf{D}_{\max}^H$  is the stiffest element,  $\boldsymbol{\eta}^E$  is the ordered SIMP interpolation function, and  $p$  is the penalty coefficient.

### Failure Criterion Identification and Ordered SIMP Stress Interpolation Strategy

The Tsai-Hill criterion is adopted here to describe the yield behavior of lattice materials. The expression of the Tsai-Hill yield criterion is:

$$\sigma^{T-H} = \left( \frac{\sigma_x}{\bar{\sigma}_x} \right)^2 + \left( \frac{\sigma_y}{\bar{\sigma}_y} \right)^2 - \frac{\sigma_x \sigma_y}{\bar{\sigma}_x \bar{\sigma}_y} + \left( \frac{\tau_{xy}}{\bar{\sigma}_{xy}} \right)^2 \leq 1. \quad (2.3)$$

where  $\bar{\sigma}_x$ ,  $\bar{\sigma}_y$ , and  $\bar{\sigma}_{xy}$  are the yield stress values for the element. In addition,  $\sigma^{T-H}$  can be expressed by the following matrix equation as:

$$\sigma^{T-H}(\rho_i) = \boldsymbol{\varepsilon}^T \mathbf{D}^T \mathbf{M} \mathbf{D} \boldsymbol{\varepsilon}, \quad (2.4)$$

where  $\boldsymbol{\varepsilon}$  is the strain and  $\mathbf{M}$  is the criterion matrix, which is given by:

$$\mathbf{M} = \begin{bmatrix} \frac{1}{\bar{\sigma}_x^2} & \frac{1}{2\bar{\sigma}_x \bar{\sigma}_y} & 0 \\ \frac{1}{2\bar{\sigma}_x \bar{\sigma}_y} & \frac{1}{\bar{\sigma}_y^2} & 0 \\ 0 & 0 & \frac{1}{\bar{\sigma}_{xy}^2} \end{bmatrix}, \quad (2.5)$$

The ordered SIMP method is applied to the stresses of the composite material. The element critical matrix is given by:

$$\mathbf{M}_e = \boldsymbol{\eta}^S \cdot \mathbf{M}_{\max}(\rho_i^T), \quad (2.6)$$

$$\boldsymbol{\eta}^S = \left( \frac{\rho_e - \rho_i^T}{\rho_{i+1}^T - \rho_i^T} \right)^p \cdot \left( \frac{\mathbf{M}_{i+1} - \mathbf{M}_i}{\mathbf{M}_{\max}} \right) + \frac{\mathbf{M}_i}{\mathbf{M}_{\max}}, \quad (2.7)$$

where  $\mathbf{M}_{\max}$  is the criterion matrix of the material which has the highest yield stress,  $\eta^S$  is the interpolation function, and  $\mathbf{M}_i$  is the criterion matrix that can be calculated by Eq. (2.5). At the microscale, the solid material consisting of a lattice structure is assumed to be isotropic with elastic perfectly plastic solid of Young's modulus of 1745 MPa, Poisson's ratio of 0.3 and yield strength of 65 MPa. The macroscale yield strength of the lattice structure is calculated at the peak of the curve of macroscopic stress versus strain. As a result, the yielding model of lattice structure can be obtained at different relative densities through the uniaxial, shear, and hydrostatic loadings under periodic boundary conditions. Eq. (2.3) gives a local constraint, which needs a high computational cost. Here, an alternative global constraint by P-norm is applied, which has the form:

$$\sigma^{T-H}_{PN} = \left( \sum_{e=1}^{Nel} (\sigma^{T-H}(\rho_e))^P \right)^{\frac{1}{P}} \leq 1, \quad (2.8)$$

where  $\sigma_{PN}$  is the global P-norm measure, P is the aggregation parameter, and Nel is the total number of elements.

### Optimization Problem Formulation

The objective function is to minimize structure weight subject to the maximum Tsai-Hill stress constraint. The optimization problem can be mathematically formulated as:

$$\left\{ \begin{array}{l} \text{find: } \boldsymbol{\rho} \\ \text{minimize: } M(\boldsymbol{\rho}) = \sum_{e=1}^{Nel} \bar{\rho}_e \\ \text{subject to: } \left\{ \begin{array}{l} \mathbf{KU} = \mathbf{F} \\ \sigma^{T-H}_{PN} \leq 1 \\ \rho_{\min} \leq \forall \bar{\rho}_e \leq 1 \end{array} \right. \end{array} \right. , \quad (2.9)$$

where  $M(\boldsymbol{\rho})$  is the objective function of the optimization problem, which represents the total mass of the structure.  $\mathbf{K}$ ,  $\mathbf{U}$  and  $\mathbf{F}$  in the equilibrium equation denote stiffness matrix, global displacement and prescribed external loads, respectively. The filtered design variable  $\forall \bar{\rho}_e$  is limited by the upper bound 1, and the lower bound  $\rho_{\min}$ . After obtaining the gradient of this model, the Method of Moving Asymptotes (MMA) is adopted to update the topological configuration iteratively.

### Case Study

#### Case 1:

The proposed method is first validated with a 2 D L-bracket benchmark case, whose boundary and loading conditions are shown in Fig. 2. For all numerical examples, 4-node quadrilateral elements are adopted. For the MMA optimizer, the default move limit is 0.5. Moreover, the initial value of design variables in the cases is set to be 0.3, and the filter radius is 3.5 element sizes. The optimization process will be converged when no further improvement of the objectives is achieved.

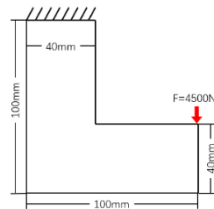




Fig. 2: Boundary and loading conditions of L-Bracket.

Structured rectangular mesh with 1st order Lagrange elements is adopted in this case. The mesh dimension is  $50 \times 50$  elements in the macroscale and  $50 \times 50$  elements in the microscale, and the

homogenized stress state is calculated at the element centroid. The two microstructures are made of isotropic material, whose yield strength is 65 MPa and Young's Modulus is 1050 MPa. The mechanical properties of the two pre-designed microstructures are listed in Tab. 1.

Microstructure 1		Density ratio	Yield strength in x direction	Yield strength in xy direction
		60%	1650	750
		$D_{11}$	$D_{12}$	$D_{33}$
		$3.8681e5$	$1.5835e5$	$8.8424e4$
Microstructure 2		Density ratio	Yield strength in x direction	Yield strength in xy direction
		40%	1250	667
		$D_{11}$	$D_{12}$	$D_{33}$
		$1.7575e5$	$1.2116e5$	$3.9591e4$

Tab. 1: Mechanical properties of two pre-designed microstructures (unit: MPa).

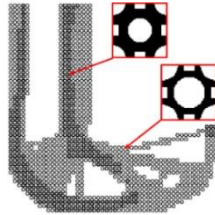


Fig. 3: Final result of full-scale design.

The optimized structure is shown in Fig. 3 with a final mass ratio of 0.2347, which proves that the lightweight structure goal is achieved. The maximum Tsai-Hill stress in microstructure 1 and microstructure 2 are 0.9482 and 0.8011, respectively, which shows better mechanical performance while alleviating structural design complexity.



Fig. 4: Tsai-Hill stress distributions for (a) microstructure 2 and (b) microstructure 1.

Fig. 4 shows the real Tsai-Hill stress distributions for different microstructure phases. It is observed that the resulting structure suffers from a significant stress concentration around the reentrant corner for microstructure 2, while the highest stress occurred at the bottom area of the bracket for microstructure 1.

*Case 2:*

The proposed approach is subsequently validated using a bone-like case, and the two microstructures listed in Tab. 1 are applied in this case.



Fig. 5: Result of bone-like case.

Fig. 5 shows the optimized bone structure, and Fig. 6 shows the real Tsai-Hill stress distributions for different microstructure phases. The optimized design's final mass ratio is 0.2644. The Fig. 6(a) part indicates microstructure 2, and the Fig.6 (b) part demonstrates microstructure 1. The maximum Tsai-Hill stresses in the two microstructures are 0.9981 and 0.8113, respectively, which depicts the real Tsai-Hill stress distributions for different microstructure phases.



Fig. 6: Tsai-Hill stress distributions for (a) microstructure 2 and (b) microstructure 1.

Conclusions

A framework for stress-based lattice structure topology optimization was proposed for additive manufacturing. The homogenization method is employed to efficiently obtain the effective mechanical properties of lattice structures in terms of relative density. Moreover, for the effective yield strength, the modified Tsai-Hill's yield criterion is applied to estimate the mechanical performance. It can be concluded that this optimization methodology can iteratively optimize the material distributions from the design domain while maintaining its mechanical properties under a given load, achieving an optimal structure with desired mechanical performance. Specifically, it considers stress constraints to ensure that the optimized structure can meet the maximum stress requirements at different scales. In addition, augmenting safety protocols is accomplished with modularized data management and enhanced structural robustness through the optimization process realized by multiscale stress-constrained ordered-SIMP interpolation. Future research will develop a modularized data link that contributes to the seamless synchronization of software information throughout organizations, especially for mass customization in additive manufacturing or, in other words, complex structure development.

Acknowledgements:

The authors would like to thank Dr. Shuzhi Xu from the University of Alberta for his help and discussions related to this work.

## References

- [1] Duncan, O.; Shepherd, T.; Moroney, C.; Foster, L.; Venkatraman, P. D.; Winwood, K.; Allen, T.; Alderson, A.: Review of auxetic materials for sports applications: Expanding options in comfort and protection, *Applied Sciences (Switzerland)* 8, 2018. <https://doi.org/10.3390/app8060941>.
- [2] Liu, J.; Gaynor, A. T.; Chen, S.; Kang, Z.; Suresh, K.; Takezawa, A.; Li, L.; Kato, J.; Tang, J.; Wang, C. C. L.; Cheng, L.; Liang, X.; To, Albert. C.: Current and future trends in topology optimization for additive manufacturing, *Structural and Multidisciplinary Optimization* 57, 2018, 2457-2483. <https://doi.org/10.1007/s00158-018-1994-3>.
- [3] Liu, J.; Ma, Y.: A survey of manufacturing oriented topology optimization methods, *Advances in Engineering Software* 100, 2016, 161-175. <https://doi.org/10.1016/j.advengsoft.2016.07.017>.
- [4] Yan, Q.; Dong, H.; Su, J.; Han, J.; Song, B.; Wei, Q.; Shi, Y.: A Review of 3D Printing Technology for Medical Applications, *Engineering* 4, 2018, 729-742. <https://doi.org/10.1016/j.eng.2018.07.021>.
- [5] Abdi, M.; Ashcroft, I.; Wildman, R. D.: Design optimisation for an additively manufactured automotive component, 2018. <https://doi.org/10.1504/IJPT.2018.090371>.
- [6] Orme, M. E.; Gschweidl, M.; Ferrari, M.; Madera, I.; Mouriaux, F.: Designing for Additive Manufacturing: Lightweighting Through Topology Optimization Enables Lunar Spacecraft, *Journal of Mechanical Design* 139, 2017. <https://doi.org/10.1115/1.4037304>.
- [7] Plocher, J.; Panesar, A.: Review on design and structural optimisation in additive manufacturing: Towards next-generation lightweight structures, *Mater Des* 183, 2019. <https://doi.org/10.1016/j.matdes.2019.108164>.
- [8] Wang, Y.; Sigmund, O.: Topology optimization of multi-material active structures to reduce energy consumption and carbon footprint, *Structural and Multidisciplinary Optimization* 67, 2024. <https://doi.org/10.1007/s00158-023-03698-3>.
- [9] Duysinx, P.; Bendsøe, M. P.: Topology optimization of continuum structures with local stress constraints, *Int J Numer Methods Eng* 43, 1998, 1453-1478. [https://doi.org/10.1002/\(SICI\)1097-0207\(19981230\)43:8<1453::AID-NME480>3.0.CO;2-2](https://doi.org/10.1002/(SICI)1097-0207(19981230)43:8<1453::AID-NME480>3.0.CO;2-2).
- [10] Conlan-Smith, C.; James, K. A.: A stress-based topology optimization method for heterogeneous structures, *Structural and Multidisciplinary Optimization* 60, 2019, 167-183. <https://doi.org/10.1007/s00158-019-02207-9>.
- [11] Xu, S.; Liu, J.; Zou, B.; Li, Q.; Ma, Y.: Stress constrained multi-material topology optimization with the ordered SIMP method, *Comput Methods Appl Mech Eng* 373, 2021, 113453. <https://doi.org/10.1016/j.cma.2020.113453>.
- [12] Han, Z.; Wei, K.; Gu, Z.; Ma, X.; Yang, X.: Stress-constrained multi-material topology optimization via an improved alternating active-phase algorithm, *Engineering Optimization* 54, 2022, 305-328. <https://doi.org/10.1080/0305215X.2020.1867119>.
- [13] Thillaithevan, D.; Bruce, P.; Santer, M.: Stress-constrained optimization using graded lattice microstructures, *Structural and Multidisciplinary Optimization* 63, 2021, 721-740. <https://doi.org/10.1007/s00158-020-02723-z>.
- [14] Wu, J.; Aage, N.; Westermann, R.; Sigmund, O.: Infill Optimization for Additive Manufacturing-Approaching Bone-Like Porous Structures, *IEEE Trans Vis Comput Graph* 24, 2018, 1127-1140. <https://doi.org/10.1109/TVCG.2017.2655523>.
- [15] Liu, X.; Shapiro, V.: Random heterogeneous materials via texture synthesis, *Comput Mater Sci* 99, 2015, 177-189. <https://doi.org/10.1016/j.commatsci.2014.12.017>.
- [16] Groen, J. P.; Sigmund, O.: Homogenization - based topology optimization for high - resolution manufacturable microstructures, *Int J Numer Methods Eng* 113, 2018, 1148-1163. <https://doi.org/10.1002/nme.5575>.
- [17] Daynes, S.; Feih, S.; Lu, W. F.; Wei, J.: Design concepts for generating optimised lattice structures aligned with strain trajectories, *Comput Methods Appl Mech Eng* 354, 2019, 689-705. <https://doi.org/10.1016/j.cma.2019.05.053>.
- [18] Daynes, S.; Feih, S.: Bio-inspired lattice structure optimisation with strain trajectory aligned trusses, *Mater Des* 213, 2022. <https://doi.org/10.1016/j.matdes.2021.110320>.